

Cosmological dynamics in R^2 gravity with logarithmic trace term

Emilio Elizalde¹, Nisha Godani² and Gauranga C. Samanta^{3*}

¹Institute of Space Sciences (IEEC-CSIC), Campus UAB,
Carrer de Can Magrans, s/n 08193 Cerdanyola del Valles, Barcelona, Spain

²Department of Mathematics, Institute of Applied Sciences and Humanities
GLA University, Mathura, Uttar Pradesh, India

³Department of Mathematics, BITS Pilani K K Birla Goa Campus, Goa, India
elizalde@ieec.uab.es; nishagodani.dei@gmail.com; gauranga81@gmail.com

Abstract

A novel function for modified gravity is proposed, $f(R, T) = R + \lambda R^2 + 2\beta \ln(T)$, with λ and β constants, R the Ricci scalar, and the energy-momentum tensor trace, T , satisfying $T = \rho - 3p > 0$. Subsequently, two equation of state parameters, namely ω and a parametric form of the Hubble parameter H , are employed in order to study the accelerated expansion and initial cosmological bounce of the corresponding universe. Hubble telescope experimental data for redshift z within the range $0.07 \leq z \leq 2.34$ are used to compare the theoretical and observational values of the Hubble parameter. Moreover, it is observed that all the energy conditions are fulfilled within a neighborhood of the bouncing point $t = 0$, what shows that the necessary condition for violation of the null energy condition, within the neighborhood of a bouncing point in general relativity, could be avoided by modifying the theory in a reasonable way. Furthermore, a large amount of negative pressure is found, which helps to understand the late time accelerated expansion phase of the universe.

Keywords: $f(R, T)$ gravity; Accelerated expansion, Energy condition, Cosmological bounce

1 Introduction

At the end of the past century, the accelerated expansion of our universe was discovered by two different cosmological surveys [1–3]. This finding was considered as one of the most important discoveries of the 20th century. Strenuous research has been going on since then, on this subject; however, the cause of this acceleration still remains unclear. New theories and modifications of the general theory of relativity have been suggested to explain the cosmic acceleration. In particular, two alternative possibilities have been intensively studied: either the universe comprises an enormous amount of dark energy, or the theory of general relativity breaks down at cosmological scales [4].

The general theory of relativity may be modified in many different ways, what is revealed by the huge number of such theories presently available in the literature [5–9]. The $f(R)$ theories of modified gravity [10] have gained ample consideration, for their capability to elucidate the accelerated expansion of the universe. In the early 1980s, already, Starobinsky [11] discussed a most simple $f(R)$ model, by taking $f(R) = R + \alpha R^2$, with $\alpha > 0$, which is considered today as representing the first ever found inflationary scenario for the universe (and one of the most natural and successful).

*Corresponding author.

$f(R)$ theories of gravity replace the scalar curvature, R , in the Einstein gravitational action by an arbitrary function, $f(R)$, with R remaining the leading order contribution to $f(R)$. Furthermore, the scenario to unify inflation with dark energy in a consistent way was proposed in [12]. A simplification of $f(R)$ gravity suggested in [13] integrates an unambiguous coupling between the matter Lagrangian and an arbitrary function of the scalar curvature, which leads to an extra force in the geodesic equation of a perfect fluid. Subsequently, it is shown that this extra force may provide a justification for the accelerated expansion of the universe [14–16]. The dynamical behavior of the matter and dark energy effects have been obtained, within extended theories of gravity, in [17–20]. Apart from that, recently many authors have studied the dynamics of cosmological models in $f(R)$ gravity from various directions [21–40]. Unsurprisingly, however, $f(R)$ theories must fulfill very strict constraints. For example, solar system tests have ruled out a good deal of the $f(R)$ models suggested so far [41]. Nevertheless, a number of realistic consistent $f(R)$ gravities which pass the solar tests were proposed in [42–44].

Apart from those, the class of $f(R, T)$ theories, where T is the trace of the stress-energy tensor [45], have gained much attention to explain the accelerated expansion of the universe. In these theories the matter term is included in the gravitational action, in which the gravitational Lagrangian density is an arbitrary function of both R and T . The random requirement on T embodies the conceivable contributions from both non-minimal coupling and unambiguous T terms.

Many functional forms for $f(R, T)$ have been studied for the derivation of cosmological dynamics in different contexts. The split-up case, $f(R, T) = f_1(R) + f_2(T)$, has received a lot of attention because it is simple and one can explore the contribution from R without specifying $f_2(T)$ and, similarly, the contribution from T without specifying $f_1(R)$. Reconstruction of $f(R, T)$ gravity in such separable theories is studied in [46]. A non-equilibrium picture of thermodynamics at the apparent horizon of the (FLRW) universe was discussed in [47]. Subsequently, many authors have been studying in depth this particular form of $f(R, T) = f_1(R) + f_2(T)$, to match different aspects of the cosmological dynamics with observations [48–76].

The motivation of this paper is to study a particularly simple but very interesting form of $f(R, T)$ gravity, indeed, the new functional form: $f(R, T) = R + \lambda R^2 + 2\beta \ln(T)$, where λ, β are constant and $T = \rho - 3p > 0$. From the above choice of $f(R, T)$, we do get to know that the term $\rho - 3p$ must be positive, in order that the function $f(R, T)$ be well defined. Therefore, the constraint $\rho - 3p > 0$ is mandatory. Subsequently, we will be able to affirm that $\rho + 3p > 0$, provided $p > 0$; now, if we are able to show in what follows that $\rho > 0$, then all energy conditions will be satisfied, i.e., the Null Energy Condition(NEC), the Weak Energy Condition(WEC), and the Strong Energy Condition(SEC) and, consequently, we will be able to assure that our model does not contain any exotic type of matter, for this particular choice of the $f(R, T)$ function.

In this paper, we use the natural system of units $G = c = 1$.

2 The background of $f(R, T)$ gravity

The $f(R, T)$ theory was first introduced, in 2011, by Harko et al. [45]. These authors extended standard general theory of relativity by modifying the gravitational Lagrangian. The gravita-

tional action in this theory is given by

$$S = S_G + S_m = \frac{1}{16\pi} \int f(R, T) \sqrt{-g} d^4x + \int \sqrt{-g} \mathcal{L} d^4x. \quad (1)$$

where $f(R, T)$ is taken to be an arbitrary function of R and T . Here R is the Ricci scalar and T is the trace of the energy momentum tensor $T_{\mu\nu}$. The matter Lagrangian density is denoted by \mathcal{L} , and the energy momentum tensor is defined in terms of the matter action as follows [77]:

$$T_{\mu\nu} = -\frac{2\delta(\sqrt{-g}\mathcal{L})}{\sqrt{-g}\delta g^{\mu\nu}}, \quad (2)$$

which yields

$$T_{\mu\nu} = g_{\mu\nu}\mathcal{L} - 2\frac{\partial\mathcal{L}}{\partial g^{\mu\nu}}. \quad (3)$$

The trace T is defined as $T = g^{\mu\nu}T_{\mu\nu}$. Let us define the variation of T with respect to the metric tensor as

$$\frac{\delta(g^{\alpha\beta}T_{\alpha\beta})}{\delta g^{\mu\nu}} = T_{\mu\nu} + \Theta_{\mu\nu}, \quad (4)$$

where $\Theta_{\mu\nu} = g^{\alpha\beta}\frac{\delta T_{\alpha\beta}}{\delta g^{\mu\nu}}$. Varying the action (1) with respect to the metric tensor $g^{\mu\nu}$, yields

$$f_R(R, T)R_{\mu\nu} - \frac{1}{2}f(R, T)g_{\mu\nu} + (g_{\mu\nu}\square - \nabla_\mu\nabla_\nu)f_R(R, T) = 8\pi T_{\mu\nu} - f_T(R, T)T_{\mu\nu} - f_T(R, T)\Theta_{\mu\nu}, \quad (5)$$

where $f_R(R, T) \equiv \frac{\partial f(R, T)}{\partial R}$ and $f_T(R, T) \equiv \frac{\partial f(R, T)}{\partial T}$. Note that, if we take $f(R, T) = R$ and $f(R, T) = f(R)$, then the equation (5) becomes simply general Einstein field equation and $f(R)$ gravity respectively. In the present work we assume that the stress-energy tensor is defined as

$$T_{\mu\nu} = (p + \rho)u_\mu u_\nu - pg_{\mu\nu}, \quad (6)$$

and the matter Lagrangian can be taken as $\mathcal{L} = -p$. The four velocity u_μ satisfies the conditions $u_\mu u^\mu = 1$ and $u^\mu\nabla_\nu u_\mu = 0$, respectively. If the matter source is a perfect fluid, then $\Theta_{\mu\nu} = -2T_{\mu\nu} - pg_{\mu\nu}$.

In this study, we shall consider $f(R, T) = f(R) + 2f(T)$, where $f(R)$ is a function of R and $f(T)$ a function of the trace of the energy momentum tensor, i.e. $T = \rho - 3p$.

3 $f(R, T) = R + \lambda R^2 + 2\beta \ln(T)$ and field equations

In this paper, the novel $f(R, T)$ function is defined as

$$f(R, T) = R + \lambda R^2 + 2\beta \ln(T), \quad (7)$$

where λ, β are constants and $T = \rho - 3p > 0$. From the above choice of $f(R, T)$, we come to know that $\rho - 3p > 0$, otherwise the function $f(R, T)$ will not be well defined. Therefore, $\rho - 3p > 0$ is mandatory. Subsequently, we can say that $\rho + 3p > 0$, provided $p > 0$; now, if we are able to show that $\rho > 0$, then all energy conditions will be satisfied, namely the Null Energy

Condition(NEC), the Weak Energy Condition(WEC), and the Strong Energy Condition(SEC). Consequently, we will be able to say that our model does not contain any exotic type of matter for this particular choice of the $f(R, T)$ function. The spacetime of the model is assumed to be the flat Fiedmann-Lemaitre-Robertson-Walker (FLRW) metric, which is defined as

$$ds^2 = dt^2 - a^2(t)(dx^2 + dy^2 + dz^2) \quad (8)$$

Using Eqs. (6), (7) and (8) in the field equation (5), the explicit form of the field equations are obtained as

$$3 \left(\frac{\dot{a}}{a} \right)^2 - \frac{18\lambda}{a^4} [\ddot{a}^2 a^2 + 2\dot{a}\ddot{a}a^2 - 5\dot{a}^4 + 2a\dot{a}^2\ddot{a}] = 8\pi\rho + 2\beta \frac{\rho + p}{\rho - 3p} - \beta \ln(\rho - 3p) \quad (9)$$

and

$$\frac{2\ddot{a}}{a} + \left(\frac{\dot{a}}{a} \right)^2 - \frac{6\lambda}{a^4} [5\dot{a}^4 - 12a\dot{a}^2\ddot{a} + a^2\ddot{a}^2 + 4a^2\dot{a}\ddot{a} + 2a^3\ddot{a}\dot{a}] = -8\pi p - \beta \ln(\rho - 3p), \quad (10)$$

where the overhead dot denotes the derivative with respect to time ‘t’.

By taking $\lambda = 0$, the field equations (9) and (10) reduce to

$$3 \left(\frac{\dot{a}}{a} \right)^2 = 8\pi\rho + \frac{2\beta(\rho + p)}{\rho - 3p} - \beta \ln(\rho - 3p) \quad (11)$$

$$\frac{2\ddot{a}}{a} + \left(\frac{\dot{a}}{a} \right)^2 = -\beta \ln(\rho - 3p) - 8\pi p \quad (12)$$

4 Model investigations

Nowadays, bouncing problem is one of the fascinating parts of the study of cosmological dynamics in modified gravity, because the big bang singularity could be avoided by a big bounce [78,79]. The indication of the bouncing universe is: the size of the scale factor contracted to a finite volume not necessarily zero, and then blows up. Subsequently, it delivers a conceivable solution to the singularity problem of the standard big bang model. To become a bounce, there must be some finite point of time at which the size of the universe attains minimum. Let us take this time to be $t = t_0$. As per the fundamental rule of differential calculus, a function ‘ f ’ attains minimum at say $t = t_0$, provided f satisfies $\dot{f}(t_0) = 0$ and $\ddot{f}(t_0) > 0$. Hence, the behavior of the scale factor at t_0 must be $\dot{a}(t_0) = 0$ and $\ddot{a}(t_0) > 0$. Precisely we can say that, if t_0 is a bounce point, then the scale factor $a(t)$ decreases, i. e. $\dot{a}(t) < 0$ for $t < t_0$ and the scale factor $a(t)$ increases, i. e. $\dot{a}(t) > 0$ for $t > t_0$, locally. Equivalently in the bouncing model the hubble parameter H runs across zero from $H < 0$ to $H > 0$ and $H = 0$ at the bouncing point. Subsequently, for bouncing problem, we must required $a(t) > a(t_0)$ for $t \neq t_0$ locally. In addition to that, the violation of Null Energy Condition (NEC) is required for a period of time inside the neighbourhood of bounce point in general relativity within the frame work of spatially flat 4-dimensional FLRW model. Furthermore, the EoS parameter ω of the matter content present in the universe must experience a phase switch from $\omega < -1$ to $\omega > -1$, to

enter into the hot big bang age after the bounce [78, 79]. Note that bounces in $f(R)$ gravity were investigated in [80–83]

The motivation of this section is to study the various cosmological dynamics under bouncing situations by defining two new equation of state (EoS) parameters and one new parametrized form of the Hubble parameter.

Let us start with a study on the possibility of obtaining the bouncing solution described by the following EoS:

$$\omega(t) = -\frac{k \ln(t + \epsilon)}{t} - 1 \quad (13)$$

where ϵ is very small and k is any arbitrary constant. We see from equation (13) that ω varies from negative infinity at $t = 0$ to the cosmological constant at $t = 1 - \epsilon$, and crosses this boundary, eventually it comes back to again cosmological constant for $t \rightarrow \infty$.

To study the bouncing solution of cosmological models, we define one more EoS as follows:

$$\omega(t) = \frac{r}{\ln t} - s \quad (14)$$

where r and s are parameter, we require $r < 0$ and $s > 0$. We see from equation (14) that ω varies from negative at $t = 0$ to the cosmological constant at $t = e^{\frac{r}{s-1}}$, and crosses this boundary, eventually it comes back to again cosmological constant for $t \rightarrow \infty$ and $s = 1$.

Now, we would like to make the parametric form of the Hubble parameter H that describes the expansion of the universe and helps us to accomplish some remarkable bouncing solutions. We parametrize the functional form of the Hubble parameter as defined as below

$$H(t) = \alpha \sin(\xi t) h(t) \quad (15)$$

where ξ , α are arbitrary constants and $h(t)$ is any smooth function. Looking at the novel proposed form of the Hubble parameter, we can observe that the trigonometric function $\sin(kt)$ vanishes at $t = 0, \frac{\pi}{k}, \frac{2\pi}{k}, \dots, \frac{n\pi}{k}$ implying that the scale factor must take a constant value at those points and the second function $h(t)$ should not vanish at those points. Now, we will have to choose $h(t)$, which could be any algebraic, rational, exponential, transcendental, or periodic, such a way that it should be smooth and non vanishing at those points. In this study, we consider a specific form of $h(t)$, which is defined as

$$h(t) = e^{\zeta t} \quad (16)$$

where ζ is any arbitrary constant. Hence, the complete parametrized form of the Hubble parameter $H(t)$ is as follows:

$$H(t) = \alpha \sin(\xi t) e^{\zeta t} \quad (17)$$

Let us assume that the universe is dominated by the matter with the EoS given by (13), we solve the field equation and obtain the corresponding evolution of scale factor $a(t)$, energy density ρ and pressure p as follows:

$$a = \kappa \exp \left(\alpha \frac{e^{\zeta t} [\zeta \sin(\xi t) - \xi \cos(\xi t)]}{\zeta^2 + \xi^2} \right) \quad (18)$$

where κ is an integration constant.

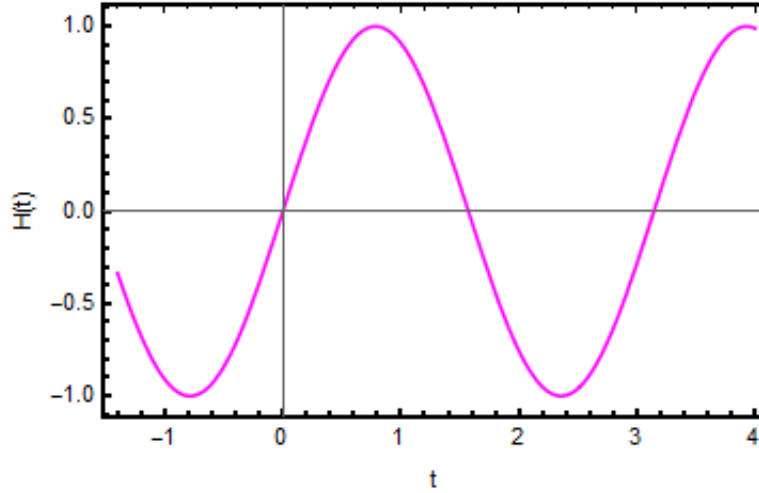


Figure 1: Hubble Parameter $H(t)$ versus t : we have considered two bouncing points, one is $t = 0$ and the second one is $t = 3.2$. At a bounce point $t = 0$, the Hubble parameter attains zero and it passes negative for $t < 0$ and positive for $t > 0$. And, the behavior of the Hubble parameter is same near the second bounce point as well.

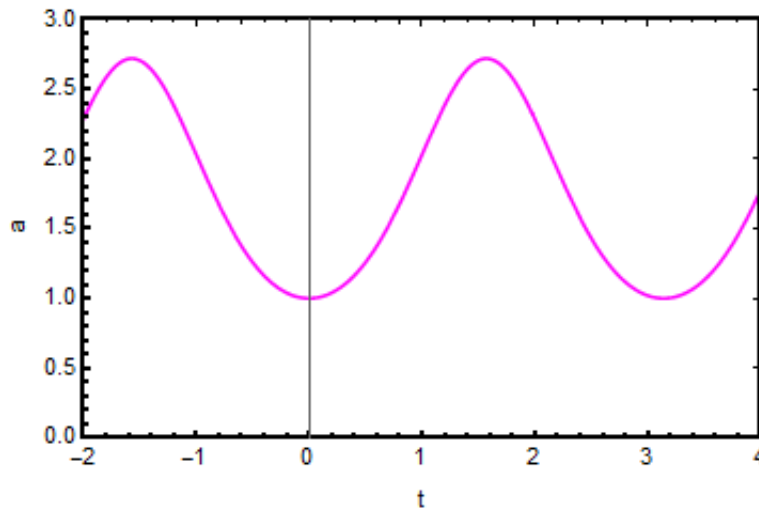


Figure 2: Scale Factor a versus t : here, we have considered two bouncing points one is $t = 0$ and the second one is $t = 3.2$. At the bounce point $t = 0$, the scale factor a attains minimum and the scale factor $a(t) > a(0)$, for $t \neq 0$, consequently, the scale factor decreases for $t < 0$, i. e. $\dot{a}(t) < 0$, for $t < 0$ and increases for $t > 0$, i. e. $\dot{a}(t) > 0$ for $t > 0$. And, the behavior of the scale factor is exactly same near the second bounce point as well.

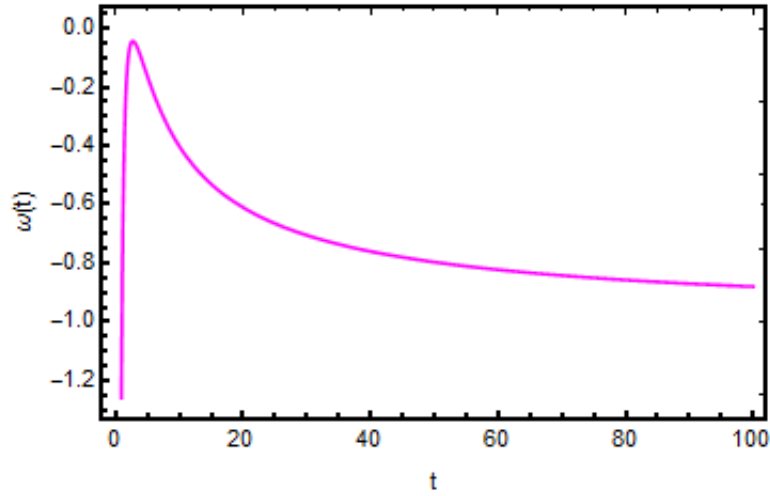


Figure 3: Equation of State Parameter $\omega(t) = -\frac{k \ln(t+\epsilon)}{t} - 1$ versus t : the value of ω tends to negative infinity at the bounce point $t = 0$, after the pounce point $t = 0$, the value of ω varies from -1 to 0 , i. e. $-1 < \omega < 0$. However, $\omega \rightarrow \infty$, for $t \rightarrow \infty$, which indicates the late time cosmic acceleration, as the universe is dominated by a cosmological constant.

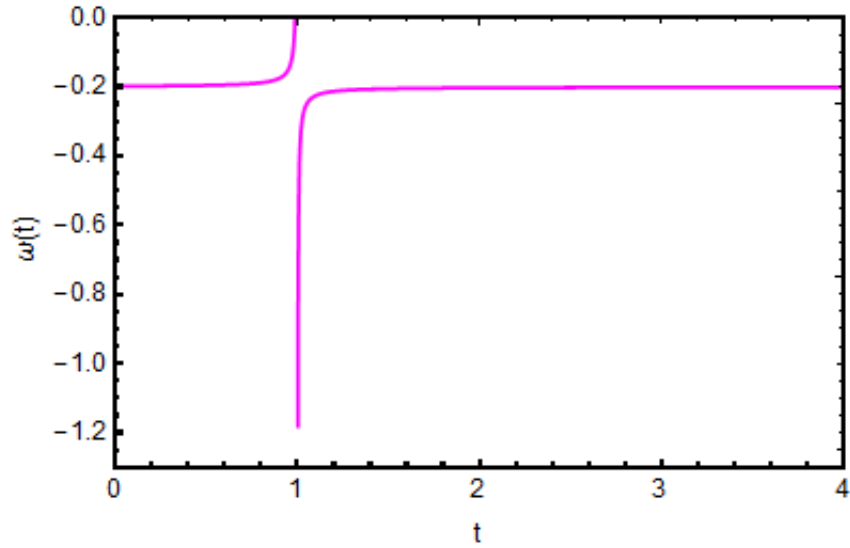


Figure 4: Equation of State Parameter $\omega(t) = \frac{r}{\ln t} - s$ versus t : the vale of the equation of sate parameter ω is lies between -1 to 0 within the neighbourhood of bouncing point $t = 0$, consequently, after the bounce point $t = 0$, the value of ω lies between -1 to 0 as well.

From Eqs. (17) and (18), we observe that the Hubble parameter $H(t)$ vanishes at $t = 0, \frac{\pi}{k}, \frac{2\pi}{k}, \dots, \frac{n\pi}{k}$, so we can choose $t = 0$ is one bounce point. One can see that our solution provides a picture of the universe evolution with contracting for $t < 0$, and then bouncing at $t = 0$ to the expanding phase for $t > 0$.

We would like to investigate the model defined in preceding section in two different cases:

Case:-I $\omega(t) = -\frac{k \ln(t+\epsilon)}{t} - 1$

Subcase:-I(a) $\lambda = 0$

$$\rho = \frac{t}{4\pi} \left[-\frac{\beta}{3k \ln(t+\epsilon) + 4t} + \frac{\alpha e^{\zeta t} (\zeta \sin(\xi t) + \xi \cos(\xi t))}{k \ln(t+\epsilon)} \right] \quad (19)$$

$$p = -\frac{(k \ln(t+\epsilon) + t)}{4\pi} \left[-\frac{\beta}{3k \ln(t+\epsilon) + 4t} + \frac{\alpha e^{\zeta t} (\zeta \sin(\xi t) + \xi \cos(\xi t))}{k \ln(t+\epsilon)} \right] \quad (20)$$

$$\rho + p = -\frac{-\frac{k\beta \ln(t+\epsilon)}{3k \ln(t+\epsilon) + 4t} + \alpha e^{\zeta t} (\zeta \sin(\xi t) + \xi \cos(\xi t))}{4\pi} \quad (21)$$

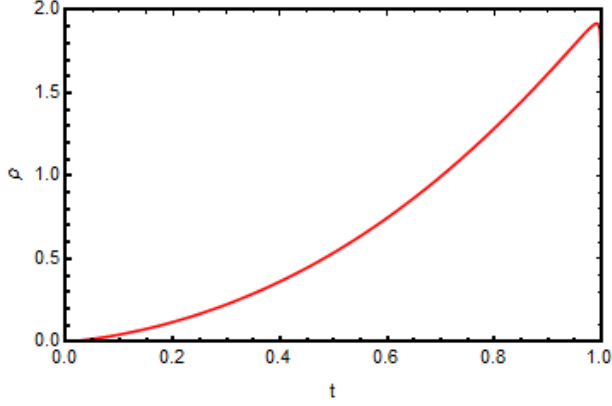
$$\rho + 3p = -\frac{(3k \ln(t+\epsilon) + 2t) (k\beta \ln(t+\epsilon) - \alpha e^{\zeta t} (3k \ln(t+\epsilon) + 4t) (\zeta \sin(\xi t) + \xi \cos(\xi t)))}{4\pi k \ln(t+\epsilon) (3k \ln(t+\epsilon) + 4t)} \quad (22)$$

$$\begin{aligned} \rho - |p| &= \frac{t}{4\pi} \left[-\frac{\beta}{3k \ln(t+\epsilon) + 4t} + \frac{\alpha e^{\zeta t} (\zeta \sin(\xi t) + \xi \cos(\xi t))}{k \ln(t+\epsilon)} \right] \\ &- \left| \frac{(k \ln(t+\epsilon) + t)}{4\pi} \left[\frac{\alpha e^{\zeta t} (\zeta \sin(\xi t) + \xi \cos(\xi t))}{k \ln(t+\epsilon)} - \frac{\beta}{3k \ln(t+\epsilon) + 4t} \right] \right| \end{aligned} \quad (23)$$

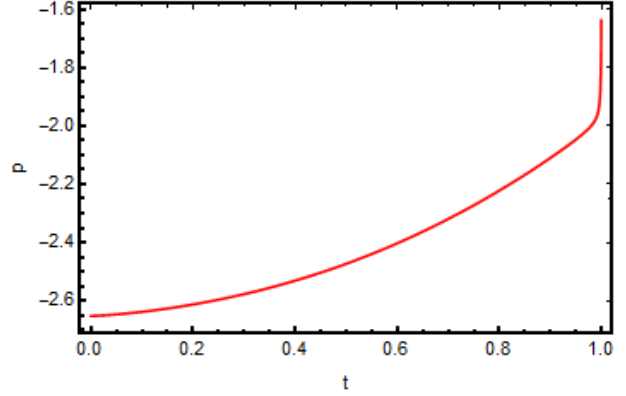
$$\rho - 3p = \frac{1}{4\pi k \log(t+\epsilon)} \left[\alpha e^{\zeta t} (3k \log(t+\epsilon) + 4t) (\zeta \sin(\xi t) + \xi \cos(\xi t)) - k\beta \log(t+\epsilon) \right] \quad (24)$$

Subcase:-I(b) $\lambda \neq 0$

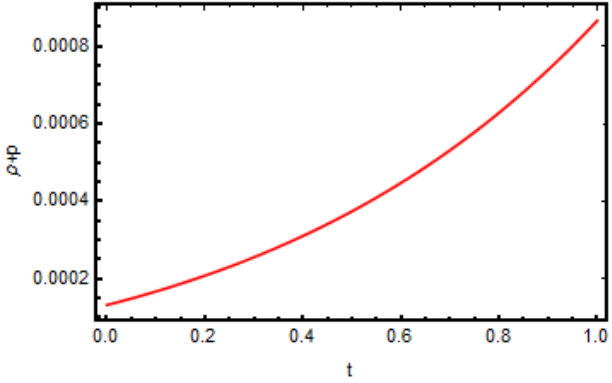
$$\begin{aligned} \rho &= \frac{t}{4\pi k \ln(t+\epsilon) (3k \ln(t+\epsilon) + 4t)} \left[48\alpha^3 \lambda e^{3\zeta t} \sin^2(\xi t) (3k \ln(t+\epsilon) + 4t) (\zeta \sin(\xi t) \right. \\ &+ \xi \cos(\xi t)) + 3\alpha^2 \lambda e^{2\zeta t} (3k \ln(t+\epsilon) + 4t) (-5\zeta^2 + \xi^2 - 10\zeta\xi \sin(2\xi t) + 5(\zeta - \xi) \\ &\times (\zeta + \xi) \cos(2\xi t)) + \alpha e^{\zeta t} (3k \ln(t+\epsilon) + 4t) (\zeta (-6\zeta^2 \lambda + 18\lambda \xi^2 + 1) \sin(\xi t) \\ &+ \xi (6\lambda (\xi^2 - 3\zeta^2) + 1) \cos(\xi t)) - \beta k \ln(t+\epsilon) \left. \right] \end{aligned} \quad (25)$$



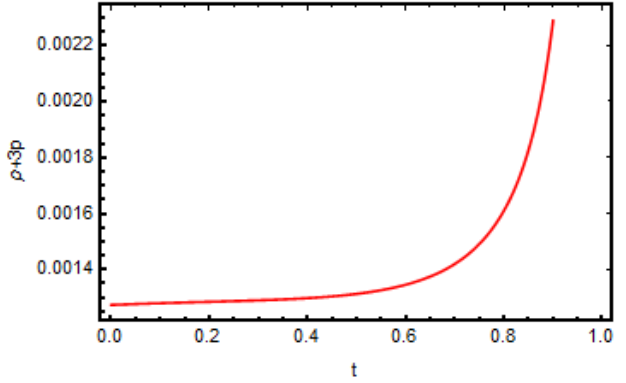
(a) Density (ρ): this figure indicates that the energy density is positive within the neighborhood of bouncing point $t = 0$.



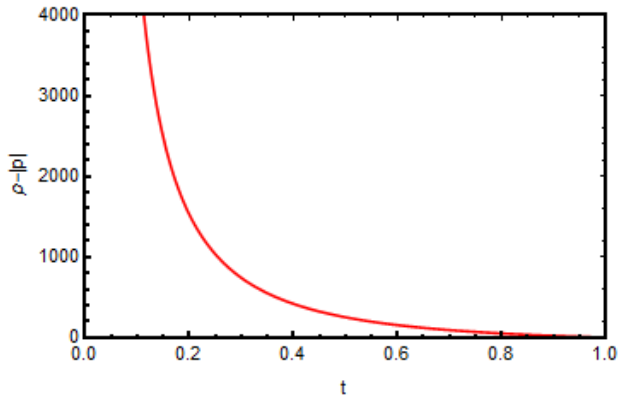
(b) Pressure (p): this figure indicates that the pressure is negative, i. e. the universe possesses a negative pressure, which could cause the accelerated expansion of the universe.



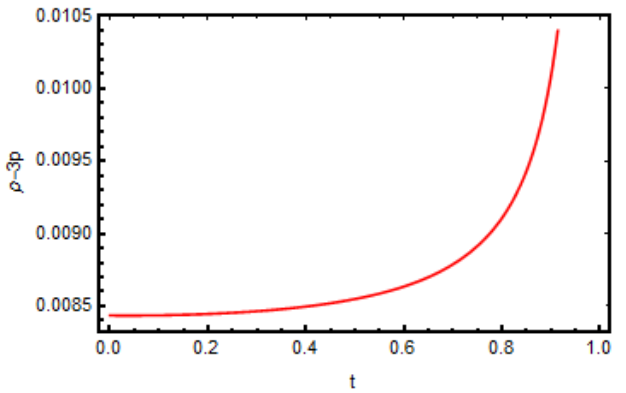
(c) NEC ($\rho + p$): it is observed that the term $\rho + p$ is positive near the bounce point $t = 0$, which indicates the NEC is satisfied. Furthermore, from the figure (a), it is shown that the energy density ρ is positive as well. Hence, we can say that the WEC is satisfied within the neighborhood of bouncing point $t = 0$.



(d) SEC ($\rho + 3p$): from the figure (c) and (d), it is observed that the terms $\rho + p > 0$ and $\rho + 3p > 0$, which indicates that the SEC is satisfied near the bounce point $t = 0$.



(e) DEC ($\rho - |p|$): for DEC, we required $\rho > 0$ and $\rho - |p| > 0$. Hence, from the figure (a) and (e), it is observed that the DEC is satisfied within the neighborhood of bouncing point $t = 0$.



(f) Stress Energy Tensor (T): from this figure it is shown that the term $\rho - 3p > 0$, which indicates that the newly defined $f(R, T)$ function is well defined.

Figure 5: Plots of Density, Pressure, NEC, SEC, DEC & Stress Energy Tensor for $\lambda = 0$ and $\omega(t) = -\frac{k \ln(t+\epsilon)}{t} - 1$

$$\begin{aligned}
p &= -\frac{(k \ln(t + \epsilon) + t)}{4\pi k \ln(t + \epsilon)(3k \ln(t + \epsilon) + 4t)} \left[48\alpha^3 \lambda e^{3\zeta t} \sin^2(\xi t)(3k \ln(t + \epsilon) + 4t)(\zeta \sin(\xi t) \right. \\
&+ \xi \cos(\xi t)) + 3\alpha^2 \lambda e^{2\zeta t}(3k \ln(t + \epsilon) + 4t) (-5\zeta^2 + \xi^2 - 10\zeta\xi \sin(2\xi t) + 5(\zeta - \xi) \\
&\times (\zeta + \xi) \cos(2\xi t)) + \alpha e^{\zeta t}(3k \ln(t + \epsilon) + 4t) (\zeta (-6\zeta^2 \lambda + 18\lambda\xi^2 + 1) \sin(\xi t) \\
&+ \xi (6\lambda (\xi^2 - 3\zeta^2) + 1) \cos(\xi t)) - \beta k \ln(t + \epsilon) \left. \right] \quad (26)
\end{aligned}$$

$$\begin{aligned}
\rho + p &= -\frac{1}{4\pi} \left[-\frac{\beta k \ln(t + \epsilon)}{3k \ln(t + \epsilon) + 4t} + 48\alpha^3 \lambda e^{3\zeta t} \sin^2(\xi t)(\zeta \sin(\xi t) + \xi \cos(\xi t)) + 3\alpha^2 \lambda e^{2\zeta t} \right. \\
&\times (-5\zeta^2 + \xi^2 - 10\zeta\xi \sin(2\xi t) + 5(\zeta - \xi)(\zeta + \xi) \cos(2\xi t)) + \alpha e^{\zeta t} (\zeta (-6\zeta^2 \lambda \\
&+ 18\lambda\xi^2 + 1) \sin(\xi t) + \xi (6\lambda (\xi^2 - 3\zeta^2) + 1) \cos(\xi t)) \left. \right] \quad (27)
\end{aligned}$$

$$\begin{aligned}
\rho + 3p &= \frac{1}{4\pi k \ln(t + \epsilon)(3k \ln(t + \epsilon) + 4t)} \left[(-3k \ln(t + \epsilon) - 2t) (48\alpha^3 \lambda e^{3\zeta t} \sin^2(\xi t) \right. \\
&\times (3k \ln(t + \epsilon) + 4t)(\zeta \sin(\xi t) + \xi \cos(\xi t)) + 3\alpha^2 \lambda e^{2\zeta t}(3k \ln(t + \epsilon) + 4t) (-5\zeta^2 \\
&+ \xi^2 - 10\zeta\xi \sin(2\xi t) + 5(\zeta - \xi)(\zeta + \xi) \cos(2\xi t)) + \alpha e^{\zeta t}(3k \ln(t + \epsilon) + 4t) \\
&\times (\zeta (-6\zeta^2 \lambda + 18\lambda\xi^2 + 1) \sin(\xi t) + \xi (6\lambda (\xi^2 - 3\zeta^2) + 1) \cos(\xi t)) \\
&- \beta k \ln(t + \epsilon) \left. \right] \quad (28)
\end{aligned}$$

$$\begin{aligned}
\rho - |p| &= \frac{t}{4\pi k \ln(t + \epsilon)(3k \ln(t + \epsilon) + 4t)} \left[48\alpha^3 \lambda e^{3\zeta t} \sin^2(\xi t)(3k \ln(t + \epsilon) + 4t)(\zeta \sin(\xi t) \right. \\
&+ \xi \cos(\xi t)) + 3\alpha^2 \lambda e^{2\zeta t}(3k \ln(t + \epsilon) + 4t) (-5\zeta^2 + \xi^2 - 10\zeta\xi \sin(2\xi t) + 5(\zeta - \xi) \\
&\times (\zeta + \xi) \cos(2\xi t)) + \alpha e^{\zeta t}(3k \ln(t + \epsilon) + 4t) (\zeta (-6\zeta^2 \lambda + 18\lambda\xi^2 + 1) \sin(\xi t) \\
&+ \xi (6\lambda (\xi^2 - 3\zeta^2) + 1) \cos(\xi t)) - \beta k \ln(t + \epsilon) \left. \right] \\
&- \left| \frac{(k \ln(t + \epsilon) + t)}{4\pi k \ln(t + \epsilon)(3k \ln(t + \epsilon) + 4t)} \left[48\alpha^3 \lambda e^{3\zeta t} \sin^2(\xi t)(3k \ln(t + \epsilon) + 4t)(\zeta \sin(\xi t) \right. \right. \\
&+ \xi \cos(\xi t)) + 3\alpha^2 \lambda e^{2\zeta t}(3k \ln(t + \epsilon) + 4t) (-5\zeta^2 + \xi^2 - 10\zeta\xi \sin(2\xi t) + 5(\zeta - \xi) \\
&\times (\zeta + \xi) \cos(2\xi t)) + \alpha e^{\zeta t}(3k \ln(t + \epsilon) + 4t) (\zeta (-6\zeta^2 \lambda + 18\lambda\xi^2 + 1) \sin(\xi t) \\
&+ \xi (6\lambda (\xi^2 - 3\zeta^2) + 1) \cos(\xi t)) - \beta k \ln(t + \epsilon) \left. \right] \left. \right| \quad (29)
\end{aligned}$$

$$\begin{aligned}
\rho - 3p &= \frac{1}{4\pi k \log(t + \epsilon)} \left[48\alpha^3 \lambda e^{3\zeta t} \sin^2(\xi t) (3k \log(t + \epsilon) + 4t) (\zeta \sin(\xi t) + \xi \cos(\xi t)) \right. \\
&+ 3\alpha^2 \lambda e^{2\zeta t} (3k \log(t + \epsilon) + 4t) (-5\zeta^2 + \xi^2 - 10\zeta\xi \sin(2\xi t) + 5(\zeta - \xi)(\zeta + \xi) \\
&\times \cos(2\xi t)) + \alpha e^{\zeta t} (3k \log(t + \epsilon) + 4t) (\zeta (-6\zeta^2 \lambda + 18\lambda \xi^2 + 1) \sin(\xi t) \\
&\left. + \xi (6\lambda (\xi^2 - 3\zeta^2) + 1) \cos(\xi t)) - \beta k \log(t + \epsilon) \right] \quad (30)
\end{aligned}$$

Case:-II $\omega(t) = \frac{r}{\ln t} - s$

Subcase:-II(a) $\lambda = 0$

$$\rho = \frac{\ln(t)}{4\pi} \left(-\frac{\alpha e^{\zeta t} (\zeta \sin(\xi t) + \xi \cos(\xi t))}{r - s \ln(t) + \ln(t)} - \frac{\beta}{-3r + 3s \ln(t) + \ln(t)} \right) \quad (31)$$

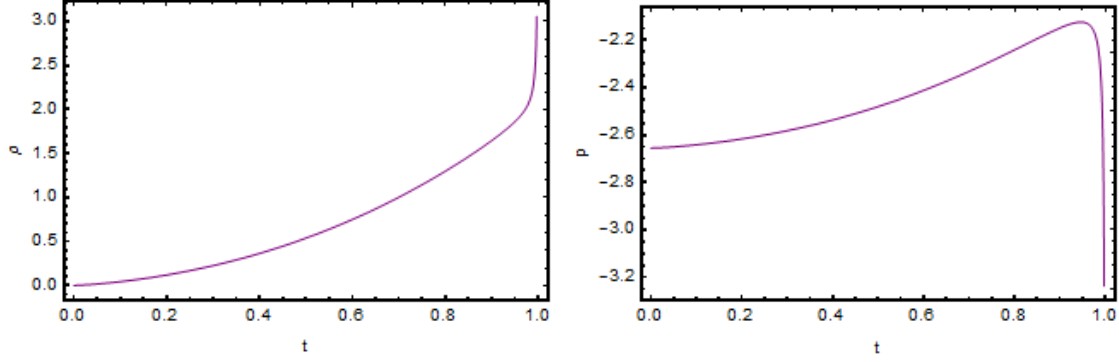
$$p = \frac{\ln(t)}{4\pi} \left(\frac{r}{\ln t} - s \right) \left(-\frac{\alpha e^{\zeta t} (\zeta \sin(\xi t) + \xi \cos(\xi t))}{r - s \ln(t) + \ln(t)} - \frac{\beta}{-3r + 3s \ln(t) + \ln(t)} \right) \quad (32)$$

$$\rho + p = \frac{\ln(t)}{4\pi} \left(1 + \frac{r}{\ln t} - s \right) \left(-\frac{\alpha e^{\zeta t} (\zeta \sin(\xi t) + \xi \cos(\xi t))}{r - s \ln(t) + \ln(t)} - \frac{\beta}{-3r + 3s \ln(t) + \ln(t)} \right) \quad (33)$$

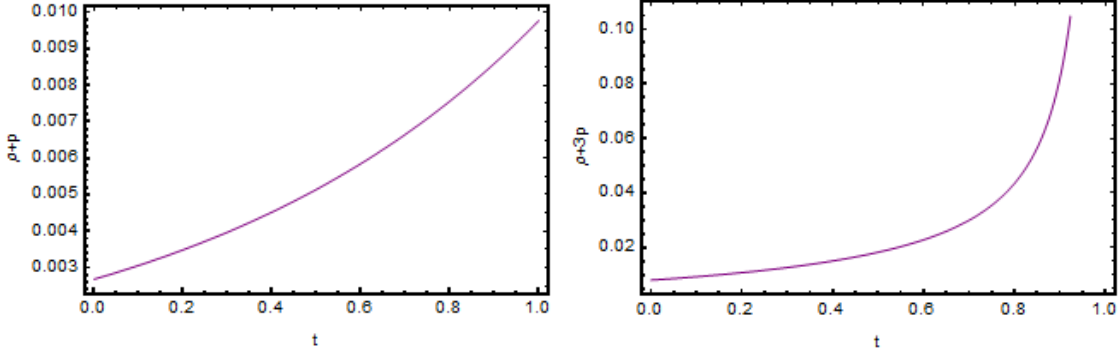
$$\begin{aligned}
\rho + 3p &= \frac{\ln(t)}{4\pi} \left(1 + 3 \left(\frac{r}{\ln t} - s \right) \right) \left(-\frac{\alpha e^{\zeta t} (\zeta \sin(\xi t) + \xi \cos(\xi t))}{r - s \ln(t) + \ln(t)} \right. \\
&\left. - \frac{\beta}{-3r + 3s \ln(t) + \ln(t)} \right) \quad (34)
\end{aligned}$$

$$\begin{aligned}
\rho - |p| &= \frac{\ln(t)}{4\pi} \left(-\frac{\alpha e^{\zeta t} (\zeta \sin(\xi t) + \xi \cos(\xi t))}{r - s \ln(t) + \ln(t)} - \frac{\beta}{-3r + 3s \ln(t) + \ln(t)} \right) \\
&- \left| \frac{\ln(t)}{4\pi} \left(\frac{r}{\ln t} - s \right) \left(-\frac{\alpha e^{\zeta t} (\zeta \sin(\xi t) + \xi \cos(\xi t))}{r - s \ln(t) + \ln(t)} - \frac{\beta}{-3r + 3s \ln(t) + \ln(t)} \right) \right| \quad (35)
\end{aligned}$$

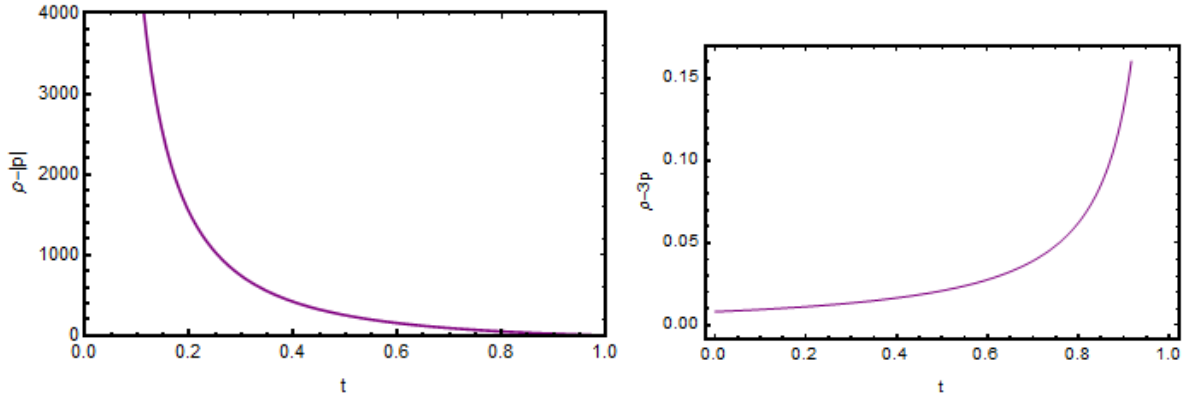
$$\begin{aligned}
\rho - 3p &= \frac{\ln(t)}{4\pi} \left(1 - 3 \left(\frac{r}{\ln t} - s \right) \right) \left(-\frac{\alpha e^{\zeta t} (\zeta \sin(\xi t) + \xi \cos(\xi t))}{r - s \ln(t) + \ln(t)} \right. \\
&\left. - \frac{\beta}{-3r + 3s \ln(t) + \ln(t)} \right) \quad (36)
\end{aligned}$$



(a) Density (ρ): from this figure, it is observed that the energy density is positive around the bouncing point $t = 0$. (b) Pressure (p): from this figure, it is observed that the pressure is negative, which could indicate the cause of accelerated expansion of the universe.

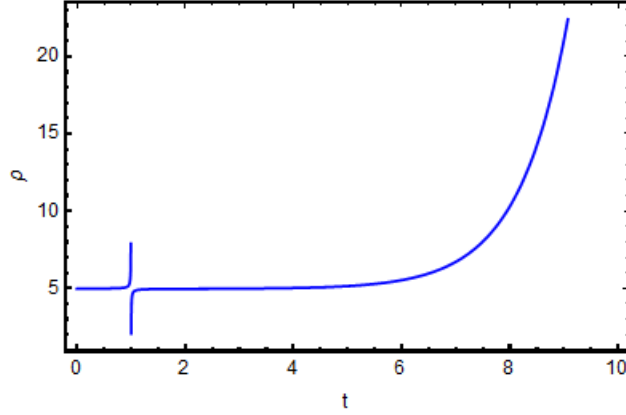


(c) NEC ($\rho + p$): from this figure, it is observed that the NEC is satisfied. Moreover, including the figure (a) and (c), we can say that WEC is satisfied as well near the bouncing point $t = 0$. (d) SEC ($\rho + 3p$): including the figure (c) and (d), we can say that SEC is satisfied within the neighborhood of bouncing point $t = 0$.

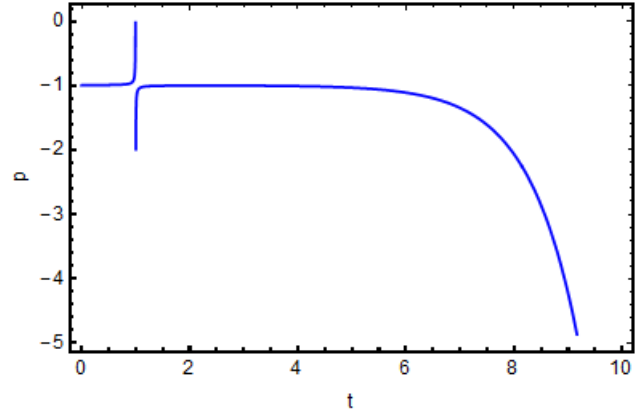


(e) DEC ($\rho - |p|$): including figure (a) and (d), we can say that DEC is satisfied within the neighborhood of bouncing point $t = 0$. (f) Stress Energy Tensor (T): from this figure, it is observed that the stress energy momentum tensor $T = \rho - 3p$ is positive, which provides the newly defined $f(R, T)$ function is well defined.

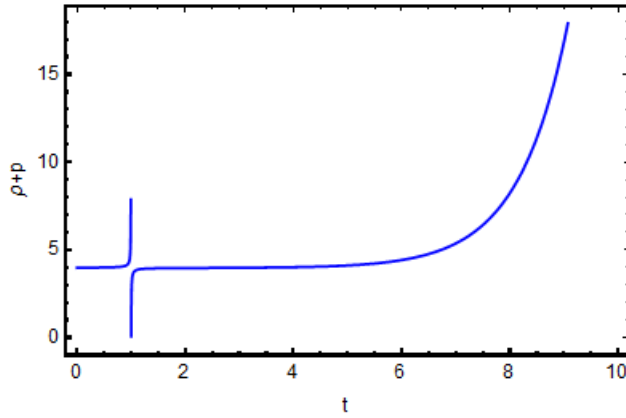
Figure 6: Plots of Density, Pressure, NEC, SEC, DEC & Stress Energy Tensor for $\lambda \neq 0$ and $\omega(t) = -\frac{k \ln(t+\epsilon)}{t} - 1$



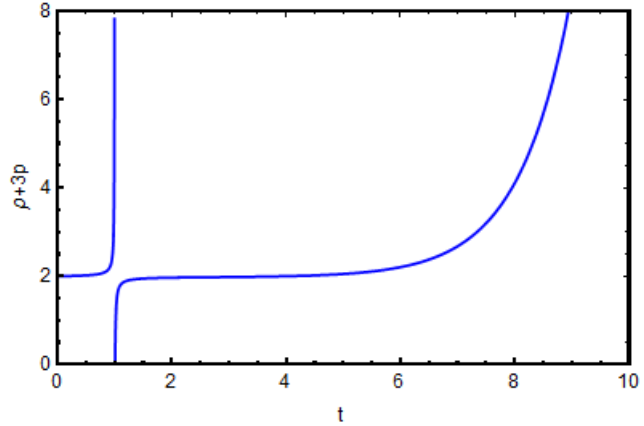
(a) Density (ρ): from the figure, it is shown that the density ρ is positive within the neighborhood of bouncing point $t = 0$. However, after the bounce point there is one discontinuous point of the graph of density, which indicates there could be one singular point.



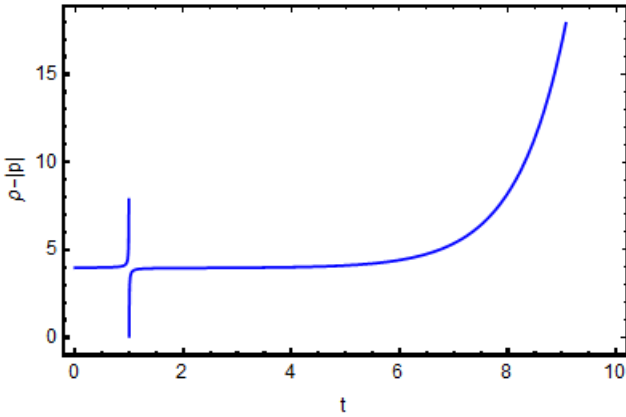
(b) Pressure (p): from the figure it is observed that the pressure is negative throughout the evolution of the universe, consequently, the pressure tends to negative infinity as time increases, which supports the accelerated expansion of the universe.



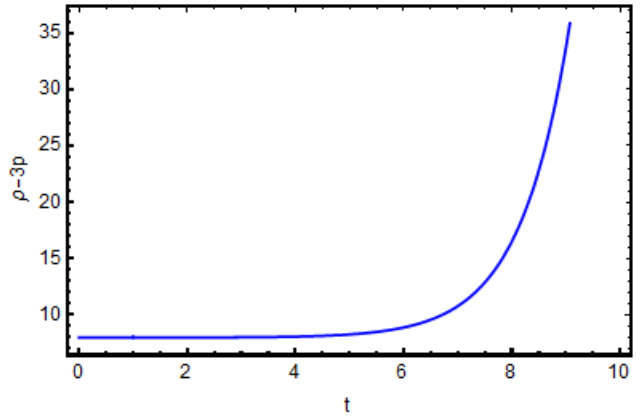
(c) NEC ($\rho + p$): from this figure, it is observed that the NEC is satisfied, subsequently, from the figure (a) and (c), we can say that the WEC condition is satisfied as well.



(d) SEC ($\rho + 3p$): we can observe from the figures (c) and (d) both $\rho + p$ and $\rho + 3p$ are positive, which provides the validation of SEC within the neighborhood of bouncing point $t = 0$.



(e) DEC ($\rho - |p|$): including figure (a) and (2), it is observed that the DEC is satisfied within the neighborhood of bouncing point $t = 0$.



(f) Stress Energy Tensor (T): this figure indicates the stress energy momentum tensor $T = \rho - 3p$ is positive throughout the evolution of the universe, which suggests the validation of $f(R, T)$ function.

Figure 7: Plots of Density, Pressure, NEC, SEC, DEC & Stress Energy Tensor for $\lambda = 0$ and $\omega(t) = \frac{r}{\ln t} - s$

Subcase:-II(b) $\lambda \neq 0$

$$\begin{aligned}
\rho &= -\frac{\log(t)}{4\pi(r - s \log(t) + \log(t))(3r - (3s + 1) \log(t))} \left[-\beta r + 48\alpha^3 \zeta \lambda e^{3\zeta t} \sin^3(\xi t) \right. \\
&\times (3r - (3s + 1) \log(t)) + \alpha e^{\zeta t} \sin(\xi t) (3r - (3s + 1) \log(t)) (-6\zeta^3 \lambda + 18\zeta \lambda \xi^2 + \zeta \\
&+ 24 \alpha^2 \lambda \xi e^{2\zeta t} \sin(2\xi t)) - 6\alpha^2 \lambda (5\zeta^2 - 3\xi^2) e^{2\zeta t} \sin^2(\xi t) (3r - (3s + 1) \log(t)) \\
&- 12\alpha^2 \lambda \xi^2 e^{2\zeta t} \cos^2(\xi t) (3r - (3s + 1) \log(t)) + \alpha \xi e^{\zeta t} (-18\zeta^2 \lambda + 6\lambda \xi^2 + 1) \cos(\xi t) \\
&\times (3r - (3s + 1) \log(t)) - 90\alpha^2 \zeta \lambda \xi r e^{2\zeta t} \sin(2\xi t) + 90\alpha^2 \zeta \lambda \xi s e^{2\zeta t} \log(t) \sin(2\xi t) \\
&\left. + \beta s \log(t) + 30\alpha^2 \zeta \lambda \xi e^{2\zeta t} \log(t) \sin(2\xi t) - \beta \log(t) \right] \tag{37}
\end{aligned}$$

$$\begin{aligned}
p &= -\frac{\log(t) \left(\frac{r}{\ln t} - s \right)}{4\pi(r - s \log(t) + \log(t))(3r - (3s + 1) \log(t))} \left[-\beta r + 48\alpha^3 \zeta \lambda e^{3\zeta t} \sin^3(\xi t) \right. \\
&\times (3r - (3s + 1) \log(t)) + \alpha e^{\zeta t} \sin(\xi t) (3r - (3s + 1) \log(t)) (-6\zeta^3 \lambda + 18\zeta \lambda \xi^2 + \zeta \\
&+ 24 \alpha^2 \lambda \xi e^{2\zeta t} \sin(2\xi t)) - 6\alpha^2 \lambda (5\zeta^2 - 3\xi^2) e^{2\zeta t} \sin^2(\xi t) (3r - (3s + 1) \log(t)) \\
&- 12\alpha^2 \lambda \xi^2 e^{2\zeta t} \cos^2(\xi t) (3r - (3s + 1) \log(t)) + \alpha \xi e^{\zeta t} (-18\zeta^2 \lambda + 6\lambda \xi^2 + 1) \cos(\xi t) \\
&\times (3r - (3s + 1) \log(t)) - 90\alpha^2 \zeta \lambda \xi r e^{2\zeta t} \sin(2\xi t) + 90\alpha^2 \zeta \lambda \xi s e^{2\zeta t} \log(t) \sin(2\xi t) \\
&\left. + \beta s \log(t) + 30\alpha^2 \zeta \lambda \xi e^{2\zeta t} \log(t) \sin(2\xi t) - \beta \log(t) \right] \tag{38}
\end{aligned}$$

$$\begin{aligned}
\rho + p &= -\frac{\log(t) \left(1 + \left(\frac{r}{\ln t} - s \right) \right)}{4\pi(r - s \log(t) + \log(t))(3r - (3s + 1) \log(t))} \left[-\beta r + 48\alpha^3 \zeta \lambda e^{3\zeta t} \sin^3(\xi t) \right. \\
&\times (3r - (3s + 1) \log(t)) + \alpha e^{\zeta t} \sin(\xi t) (3r - (3s + 1) \log(t)) (-6\zeta^3 \lambda + 18\zeta \lambda \xi^2 + \zeta \\
&+ 24 \alpha^2 \lambda \xi e^{2\zeta t} \sin(2\xi t)) - 6\alpha^2 \lambda (5\zeta^2 - 3\xi^2) e^{2\zeta t} \sin^2(\xi t) (3r - (3s + 1) \log(t)) \\
&- 12\alpha^2 \lambda \xi^2 e^{2\zeta t} \cos^2(\xi t) (3r - (3s + 1) \log(t)) + \alpha \xi e^{\zeta t} (-18\zeta^2 \lambda + 6\lambda \xi^2 + 1) \cos(\xi t) \\
&\times (3r - (3s + 1) \log(t)) - 90\alpha^2 \zeta \lambda \xi r e^{2\zeta t} \sin(2\xi t) + 90\alpha^2 \zeta \lambda \xi s e^{2\zeta t} \log(t) \sin(2\xi t) \\
&\left. + \beta s \log(t) + 30\alpha^2 \zeta \lambda \xi e^{2\zeta t} \log(t) \sin(2\xi t) - \beta \log(t) \right] \tag{39}
\end{aligned}$$

$$\begin{aligned}
\rho + 3p &= -\frac{\log(t) \left(1 + 3 \left(\frac{r}{\ln t} - s \right) \right)}{4\pi(r - s \log(t) + \log(t))(3r - (3s + 1) \log(t))} \left[-\beta r + 48\alpha^3 \zeta \lambda e^{3\zeta t} \sin^3(\xi t) \right. \\
&\times (3r - (3s + 1) \log(t)) + \alpha e^{\zeta t} \sin(\xi t) (3r - (3s + 1) \log(t)) (-6\zeta^3 \lambda + 18\zeta \lambda \xi^2 + \zeta \\
&+ 24 \alpha^2 \lambda \xi e^{2\zeta t} \sin(2\xi t)) - 6\alpha^2 \lambda (5\zeta^2 - 3\xi^2) e^{2\zeta t} \sin^2(\xi t) (3r - (3s + 1) \log(t)) \\
&- 12\alpha^2 \lambda \xi^2 e^{2\zeta t} \cos^2(\xi t) (3r - (3s + 1) \log(t)) + \alpha \xi e^{\zeta t} (-18\zeta^2 \lambda + 6\lambda \xi^2 + 1) \cos(\xi t) \\
&\times (3r - (3s + 1) \log(t)) - 90\alpha^2 \zeta \lambda \xi r e^{2\zeta t} \sin(2\xi t) + 90\alpha^2 \zeta \lambda \xi s e^{2\zeta t} \log(t) \sin(2\xi t) \\
&\left. + \beta s \log(t) + 30\alpha^2 \zeta \lambda \xi e^{2\zeta t} \log(t) \sin(2\xi t) - \beta \log(t) \right] \tag{40}
\end{aligned}$$

$$\begin{aligned}
\rho - |p| &= -\frac{\log(t)}{4\pi(r - s \log(t) + \log(t))(3r - (3s + 1) \log(t))} \left[-\beta r + 48\alpha^3 \zeta \lambda e^{3\zeta t} \sin^3(\xi t) \right. \\
&\times (3r - (3s + 1) \log(t)) + \alpha e^{\zeta t} \sin(\xi t) (3r - (3s + 1) \log(t)) (-6\zeta^3 \lambda + 18\zeta \lambda \xi^2 + \zeta \\
&+ 24 \alpha^2 \lambda \xi e^{2\zeta t} \sin(2\xi t)) - 6\alpha^2 \lambda (5\zeta^2 - 3\xi^2) e^{2\zeta t} \sin^2(\xi t) (3r - (3s + 1) \log(t)) \\
&- 12\alpha^2 \lambda \xi^2 e^{2\zeta t} \cos^2(\xi t) (3r - (3s + 1) \log(t)) + \alpha \xi e^{\zeta t} (-18\zeta^2 \lambda + 6\lambda \xi^2 + 1) \cos(\xi t) \\
&\times (3r - (3s + 1) \log(t)) - 90\alpha^2 \zeta \lambda \xi r e^{2\zeta t} \sin(2\xi t) + 90\alpha^2 \zeta \lambda \xi s e^{2\zeta t} \log(t) \sin(2\xi t) \\
&+ \beta s \log(t) + 30\alpha^2 \zeta \lambda \xi e^{2\zeta t} \log(t) \sin(2\xi t) - \beta \log(t) \left. \right] \\
&- \left| \frac{\log(t) \left(\frac{r}{\ln t} - s \right)}{4\pi(r - s \log(t) + \log(t))(3r - (3s + 1) \log(t))} \left[-\beta r + 48\alpha^3 \zeta \lambda e^{3\zeta t} \sin^3(\xi t) \right. \right. \\
&\times (3r - (3s + 1) \log(t)) + \alpha e^{\zeta t} \sin(\xi t) (3r - (3s + 1) \log(t)) (-6\zeta^3 \lambda + 18\zeta \lambda \xi^2 + \zeta \\
&+ 24 \alpha^2 \lambda \xi e^{2\zeta t} \sin(2\xi t)) - 6\alpha^2 \lambda (5\zeta^2 - 3\xi^2) e^{2\zeta t} \sin^2(\xi t) (3r - (3s + 1) \log(t)) \\
&- 12\alpha^2 \lambda \xi^2 e^{2\zeta t} \cos^2(\xi t) (3r - (3s + 1) \log(t)) + \alpha \xi e^{\zeta t} (-18\zeta^2 \lambda + 6\lambda \xi^2 + 1) \cos(\xi t) \\
&\times (3r - (3s + 1) \log(t)) - 90\alpha^2 \zeta \lambda \xi r e^{2\zeta t} \sin(2\xi t) + 90\alpha^2 \zeta \lambda \xi s e^{2\zeta t} \log(t) \sin(2\xi t) \\
&+ \beta s \log(t) + 30\alpha^2 \zeta \lambda \xi e^{2\zeta t} \log(t) \sin(2\xi t) - \beta \log(t) \left. \right] \left| \right. \quad (41)
\end{aligned}$$

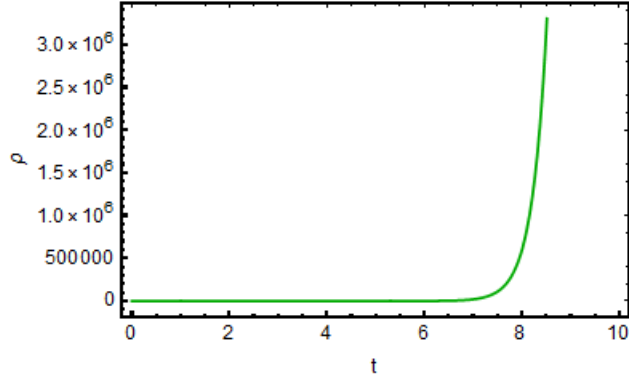
$$\begin{aligned}
\rho - 3p &= -\frac{\log(t) \left(1 - 3 \left(\frac{r}{\ln t} - s \right) \right)}{4\pi(r - s \log(t) + \log(t))(3r - (3s + 1) \log(t))} \left[-\beta r + 48\alpha^3 \zeta \lambda e^{3\zeta t} \sin^3(\xi t) \right. \\
&\times (3r - (3s + 1) \log(t)) + \alpha e^{\zeta t} \sin(\xi t) (3r - (3s + 1) \log(t)) (-6\zeta^3 \lambda + 18\zeta \lambda \xi^2 + \zeta \\
&+ 24 \alpha^2 \lambda \xi e^{2\zeta t} \sin(2\xi t)) - 6\alpha^2 \lambda (5\zeta^2 - 3\xi^2) e^{2\zeta t} \sin^2(\xi t) (3r - (3s + 1) \log(t)) \\
&- 12\alpha^2 \lambda \xi^2 e^{2\zeta t} \cos^2(\xi t) (3r - (3s + 1) \log(t)) + \alpha \xi e^{\zeta t} (-18\zeta^2 \lambda + 6\lambda \xi^2 + 1) \cos(\xi t) \\
&\times (3r - (3s + 1) \log(t)) - 90\alpha^2 \zeta \lambda \xi r e^{2\zeta t} \sin(2\xi t) + 90\alpha^2 \zeta \lambda \xi s e^{2\zeta t} \log(t) \sin(2\xi t) \\
&+ \beta s \log(t) + 30\alpha^2 \zeta \lambda \xi e^{2\zeta t} \log(t) \sin(2\xi t) - \beta \log(t) \left. \right] \quad (42)
\end{aligned}$$

5 Hubble parameter versus redshift

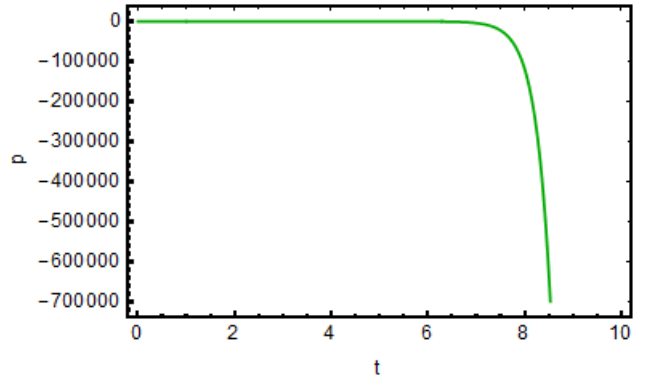
In the present section, a differential equation for Hubble parameter with respect to redshift is obtained. The values of the parameters present in the differential equation are estimated using the χ^2 test. Then, the differential equation is solved and theoretical values of the Hubble parameter are calculated. Further, the theoretical and observational values of the Hubble parameter are compared.

Differentiating (17) with respect to t ,

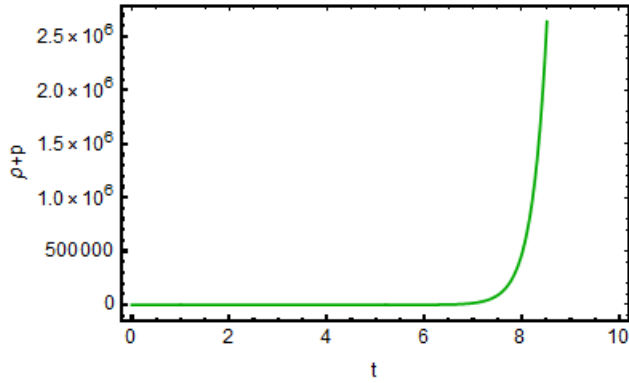
$$\frac{dH}{dt} = \alpha e^{\zeta t} (\xi \cos \xi t + \zeta \sin \xi t). \quad (43)$$



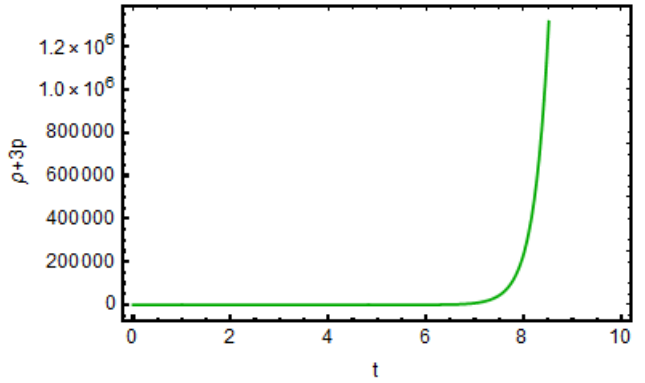
(a) Density (ρ): the behaviour of the energy density is positive within the neighbourhood of bouncing point $t = 0$.



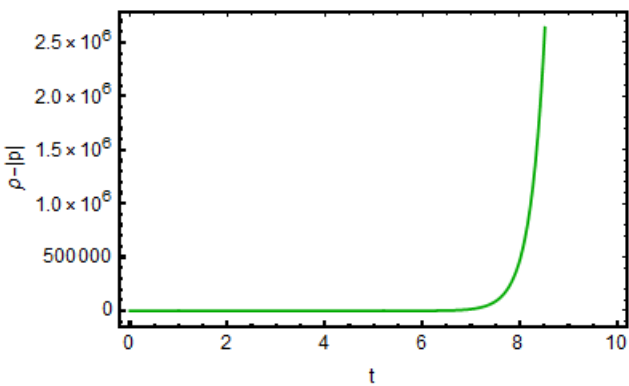
(b) Pressure (p): the behaviour of the pressure is negative within the neighbourhood of bouncing point and consequently, decreases to negative infinity, which causes the late time accelerated expansion of the universe.



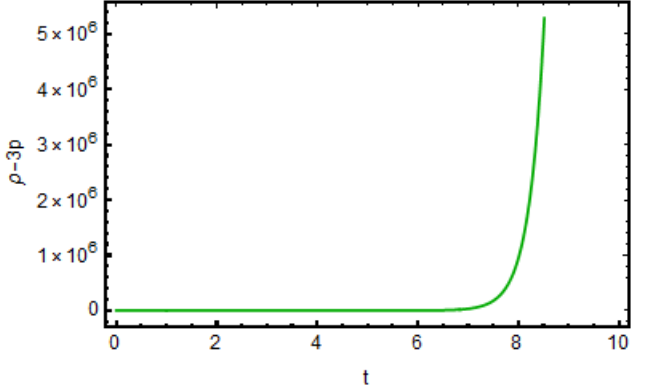
(c) NEC ($\rho + p$): from the figure it is shown that $\rho + p > 0$, which indicates the NEC is satisfied near the bouncing point, subsequently, from the figure (a), we can see that the energy density ρ is positive, hence the WEC is satisfied as well within the neighbourhood of bouncing point.



(d) SEC ($\rho + 3p$): this figure indicates $\rho + 3p > 0$ near the bounce point $t = 0$. From the figure (c) and (d), we can say that $\rho + p > 0$ and $\rho + 3p > 0$, which indicates the SEC is satisfied within the neighbourhood of bouncing point.



(e) DEC ($\rho - |p|$): from the figure (a) and (e), we confirmed that the DEC is satisfied within the neighbourhood of bouncing point $t = 0$.



(f) Stress Energy Tensor (T): from this figure it is observed that $T = \rho - 3p > 0$, which indicates our newly defined $f(R, T)$ function is we defined.

Figure 8: Plots of Density, Pressure, NEC, SEC, DEC & Stress Energy Tensor for $\lambda \neq 0$ and $\omega(t) = \frac{r}{\ln t} - s$

From Eq. (43) and using relation $1 + z = \frac{a_0}{a}$, we obtained

$$(1 + z)H(z)\frac{dH(z)}{dz} + \zeta H(z) = -\alpha\xi e^{\zeta t} \cos \xi t. \quad (44)$$

Now, using Eqns. (17) and (18), we get

$$(1 + z)H(z)\frac{dH(z)}{dz} + 2\zeta H(z) + (\xi^2 + \zeta^2) \ln(1 + z) = 0. \quad (45)$$

The differential equation (45) contains two parameters ζ and ξ . The values of these parameters are obtained by minimizing

$$\chi^2(\zeta, \xi) = \sum_{i=1}^{29} \frac{[H_{th}(\zeta, \xi; z_i) - H_{obs}(z_i)]^2}{\sigma_{H(z_i)}^2}, \quad (46)$$

where H_{th} and H_{obs} denote theoretical and observed values of Hubble parameter respectively and $\sigma_{H(z_i)}$ denote standard error for each observed value. The present value of Hubble parameter is considered as $H_0 = 67.8$ Km/s/Mpc [84]. 29 observational Hubble parameter data are taken from [85–92]. In ζ – ξ plane the likelihood contours for 1σ , 2σ and 3σ errors are drawn in Fig. (9). The values of parameters ζ and ξ are found to be equal to -46 and 1.6 respectively for minimum value 123.567 of χ^2 . For $\zeta = -46$ and $\xi = 1.6$, the numerical solution of non-linear differential equation (45) is obtained and plotted in Fig. (10) with respect to red shift through a continuous curve. In this figure, bars show the error between theoretical and observational values of Hubble parameter. Clearly, it represents a good fit to the experimental Hubble parameter data with $\zeta = -46$ and $\xi = 1.6$. Thus, it enhances the importance of the newly defined Hubble parameter for the present model.

6 Results and discussion

This work was aimed at studying the cosmological dynamics under a bouncing scenario within the framework of a spatially flat 4-dimensional FLRW model in a $f(R, T)$ theory of gravity. The $f(R, T)$ function is here defined as $f(R, T) = R + \lambda R^2 + 2\beta \ln(T)$, where λ and β are constant and $T = \rho - 3p > 0$. A parametric form of the Hubble parameter was also proposed here, as $H(t) = \alpha \sin(\xi t)e^{\zeta t}$, where α , ξ and ζ are arbitrary constants. Consequently, the scale factor has been obtained as $a(t) = \kappa \exp\left(\alpha \frac{e^{\zeta t}[\zeta \sin(\xi t) - \xi \cos(\xi t)]}{\zeta^2 + \xi^2}\right)$, where κ is an integration constant.

Since $H(t)$ vanishes at $t = 0, \frac{\pi}{k}, \frac{2\pi}{k}, \dots, \frac{n\pi}{k}$, the point $t = 0$ is chosen as a first bouncing point. The Hubble parameter is plotted in Fig.(1). In the neighborhood of the bouncing point, we can observe a contraction phase for $t < 0$, the bounce at $t = 0$, and an expansion phase for $t > 0$. The scale factor is normalized as $a = 1$ at the bouncing point. In Fig. (2), in the neighborhood of the bouncing point the scale factor is shown to decrease, for $t < 0$, and to increase, for $t > 0$. Thus, the scale factor gets its non-zero and minimum value at $t = 0$.

Moreover, two forms of the EoS parameter were defined. The first form is $\omega(t) = -\frac{k \ln(t+\epsilon)}{t} - 1$, where ϵ is very small and k is an arbitrary constant. It was plotted in Fig. (3) with respect to t .

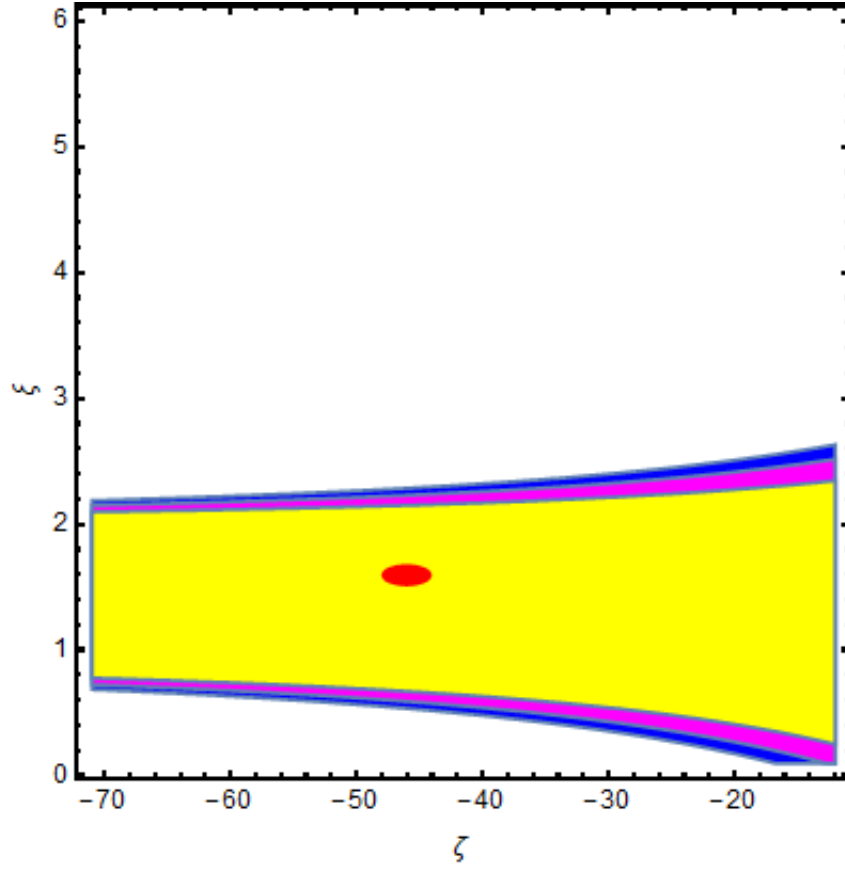


Figure 9: 1σ (yellow shaded), 2σ (magenta shaded) and 3σ (blue shaded) likelihood contours in $\zeta - \xi$ plane.

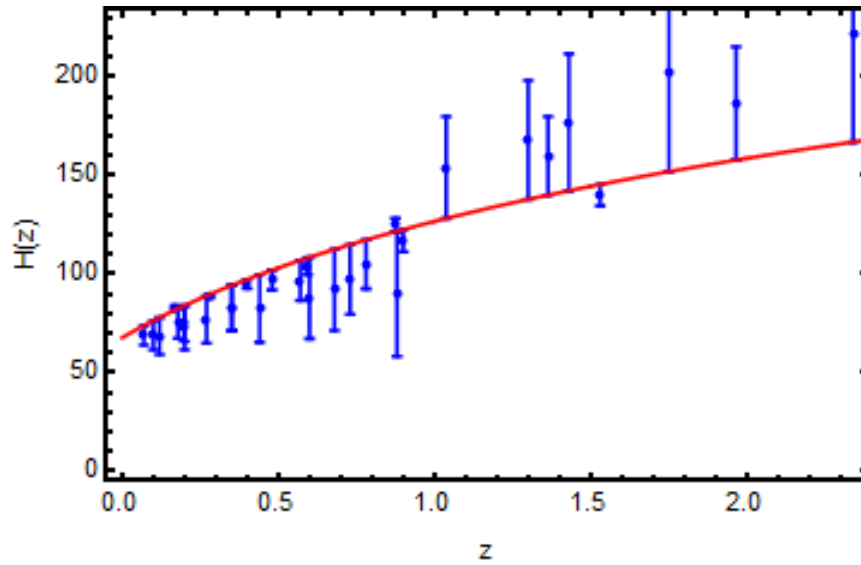


Figure 10: Hubble Parameter $H(z)$ versus z : we have considered present value of Hubble parameter equal to 67.8 Km/s/Mpc and 31 observed Hubble data.

As t increases from 0 to $1 - \epsilon$, $\omega(t)$ increases from $-\infty$ to -1 . Further, as t increases from $1 - \epsilon$ to 2.72, $\omega(t)$ increases towards -0.0436542 , after what it decreases and approaches the value -1 as t tends to infinity, which indicates that the universe is dominated by a cosmological constant at late time. Consequently, the late time accelerated expansion stage of the universe can be naturally realized in this model. The second form of $\omega(t)$ is defined as $\omega(t) = \frac{r}{\ln t} - s$, where r and s are constants, with $r < 0$ and $s > 0$. It is plotted in Fig. (4) with respect to t where $\omega(t)$ is shown to vary from a negative value at $t = 0$ to the cosmological constant at $t = 1.00313$.

Using the background of $f(R, T)$ gravity, the Einstein's field equations were derived and, using the EoS parameters discussed above, these equations have been solved. The energy density ρ , pressure p , and the stress energy tensor $T = \rho - 3p$ have been calculated. In addition to these, various combinations of ρ and p , used in the following energy conditions, have been determined:

- (i) Null energy condition (NEC): $\text{NEC} \Leftrightarrow \rho + p \geq 0$
- (ii) Weak energy condition (WEC): $\text{WEC} \Leftrightarrow \rho \geq 0, \rho + p \geq 0$
- (iii) Strong energy condition (SEC): $\text{SEC} \Leftrightarrow \rho + p \geq 0, \rho + 3p \geq 0$
- (iv) Dominant energy condition (DEC): $\text{DEC} \Leftrightarrow \rho \geq 0, \rho - |p| \geq 0$

For each EoS parameter, the computation was performed in two subcases (a) $\lambda = 0$ and (b) $\lambda \neq 0$. Summarizing, we have two cases: Case I: $\omega(t) = -\frac{k \ln(t+\epsilon)}{t} - 1$ with subcases: I(a) $\lambda = 0$ & I(b) $\lambda \neq 0$ and Case II: $\omega(t) = \frac{r}{\ln t} - s$ with subcases: II(a) $\lambda = 0$ & II(b) $\lambda \neq 0$. In Subcases I(a) and I(b), the terms ρ , p , $\rho + p$, $\rho + 3p$, $\rho - |p|$ and $\rho - 3p$ are plotted for the variation of t near the neighbourhood of bouncing point $t = 0$, i. e. from 0 to $1 - \epsilon$ in Figs. (5) & (6) respectively. Similarly, in Subcases II(a) and II(b), the results are plotted for the variation of t from 0 to 10 in Figs. (7) & (8) respectively. In each subcase, ρ , $\rho + p$, $\rho + 3p$, $\rho - |p|$ and $\rho - 3p$ are found to be positive. The positivity of $\rho - 3p$ is necessary for the $f(R, T)$ function to be well defined and the positivity of ρ , $\rho + p$, $\rho + 3p$ and $\rho - |p|$ represents the absence of exotic matter in our model, i.e. it is only filled with normal matter satisfying the energy conditions. Furthermore, the pressure p is found to be negative, which implies gravitational repulsion during the accelerating phase, in concordance with the astronomical observations.

In short, by defining appropriate forms of the EOS parameter, the Hubble parameter and the $f(R, T)$ function, we have found the existence of a bouncing universe free from exotic matter and having a non-vanishing and minimum scale factor at the bouncing point.

7 Conclusions

In the present paper, the non-singular bounce in spatially flat 4-dimensional FLRW model has been explored by working with two EoS parameters and one novel parametric form of the Hubble parameter. Einstein's field equations have been obtained in the framework of $f(R, T)$ gravity with a newly proposed $f(R, T) = R + \lambda R^2 + 2\beta \ln(T)$ function, where the condition $T = \rho - 3p > 0$ was required, so that the function $f(R, T)$ is well defined. From Figs. 5(f), 6(f), 7(f), and 8(f), it is observed that the stress energy momentum tensor $T = \rho - 3p$ is positive. Hence, it turns out that our new function is well defined and its consistency is justified.

Usually, for general relativity, within the framework of the spatially flat 4-dimensional FLRW

model, violation of the Null Energy Condition (NEC) is unavoidable for a period of time inside the neighbourhood of the bounce point [78,79]. However, in the present study, we have obtained that all the energy conditions are satisfied within a neighborhood of the bouncing point, $t = 0$. Therefore, we reach here the interesting conclusion that the violation of the NEC is not always a necessary condition in modified gravity theories; at the very least, for the particular form of theory here considered, $f(R, T) = R + \lambda R^2 + 2\beta \ln(T)$, it can be avoided.

Moreover, it is interesting to note that pressure is negative within the neighborhood of the bouncing point and, subsequently, it decreases to negative infinity throughout the evolution, which indicates that the universe may evolve indeed to a huge negative pressure stage. This negative pressure helps us to naturally realize the late time accelerated expansion of our universe. The best fit to the experimental results for the Hubble parameter for different redshifts is determined for these values of the parameters here: $\zeta = -46$ and $\xi = 1.6$.

Acknowledgements. This work was partially supported by MINECO (Spain), FIS2016-76363-P, by the CPAN Consolider Ingenio 2010 Project, and by AGAUR (Catalan Government), project 2017-SGR-247.

References

- [1] A. G. Riess, et al., *Astron. J* **116** (1998) 1009.
- [2] S. Perlmutter, et al., *Nature* **391** (1998) 51.
- [3] S. Perlmutter, et al., *Astrophys. J.* **517** (1999) 565.
- [4] J. A. Frieman, M. S. Turner and D. Huterer, *Annu. Rev. Astron. Astrophys.* **46** (2008) 385.
- [5] S. Capozziello and M. de Laurentis, *Phys. Rep.* **509** (2011) 167.
- [6] S. Nojiri and S. D. Odintsov, *Phys. Rept.* **505** (2011) 59.
- [7] T. Clifton, P. G. Ferreira, A. Padilla and C. Skordis, *Physics Reports* **513** (2012) 1.
- [8] E. Berti, et al., *Classical Quant. Grav.* **32** (2015) 243001.
- [9] S. Nojiri, S. D. Odintsov and V. K. Oikonomou, *Phys. Rept.* **692** (2017) 1.
- [10] H. A. Buchdahl, *Mon. Not. R. Astron. Soc.* **150** (1970) 1.
- [11] A. A. Starobinsky, *Phys. Lett. B* **91** (1980) 99.
- [12] S. Nojiri and S. D. Odintsov, *Phys. Rev. D* **68** (2003) 123512.
- [13] O. Bertolami, C. G. Boehmer, T. Harko and F. S. N. Lobo, *Phys. Rev. D* **75** (2007) 104016.
- [14] S. Nojiri and S. D. Odintsov, *Int. J. Geom. Methods Mod. Phys.* **4** (2007) 115.
- [15] O. Bertolami, P. Frazão and J. Páramos, *Phys. Rev. D* **81** (2010) 104046.

- [16] K. Bamba, S. Capozziello, S. Nojiri and S. D. Odintsov, *Astrophys. Space Sci.* **342** (2012) 155.
- [17] S. Nojiri, S. D. Odintsov and M. Sami, *Phys. Rev. D* **74** (2006) 046004.
- [18] Y. Shirasaki, Y. Komiya, M. Ohishi and Y. Mizumoto *Publ. Astron. Soc. Jap.* **68** (2016) 23.
- [19] S. Capozziello, T. Harko, T. S. Koivisto, F. S. N. Lobo and G. J. Olmo *J. Cosm. Astrop. Phys.* **2013** (2013) 024.
- [20] D. C. Rodrigues, P. L. de Oliveira, J. C. Fabris and G. Gentile *Month. Not. Roy. Astron. Soc.* **445** (2014) 3823.
- [21] S. Capozziello, C. A. Mantica and L. G. Molinari, *Int. J. Geom. Meth. Mod. Phys.* **16** (2018) 1950008.
- [22] N. Godani and G. C. Samanta, *Int. J. Mod. Phys. D* **28** (2018) 1950039.
- [23] F. Bombacigno and G. Montani, *Eur. Phys. J. C* **79** (2019) 405.
- [24] F. Sbisà, O. F. Piattella and S. E. Jorás, *Phys. Rev. D* **99** (2019) 104046.
- [25] L. Chen, *Phys. Rev. D* **99** (2019) 064025.
- [26] E. Elizalde, S. D. Odintsov, V. K. Oikonomou and T. Paul, *JCAP* **1902** (2019) 017.
- [27] E. Elizalde, S. D. Odintsov, T. Paul and D. Sáez-Chillón Gómez, *Phys. Rev. D* **99** (2019) 063506.
- [28] A. V. Astashenok, K. Mosani, S. D. Odintsov and G. C. Samanta, *Int. J. Geom. Meth. Mod. Phys.* **16** (2019) 1950035.
- [29] T. Miranda, C. Escamilla-Rivera, O. F. Piattella and J. C. Fabris, *JCAP* **2019** (2019) 028.
- [30] J. R. Nascimento, G. J. Olmo, P. J. Porfirio, A. Yu. Petrov and A. R. Soares, *Phys. Rev. D* **99** (2019) 064053.
- [31] S. D. Odintsov and V. K. Oikonomou, *Phys. Rev. D* **99** (2019) 064049.
- [32] E. Elizalde, S. Nojiri and S. D. Odintsov, *Phys. Rev. D* **70**, 043539 (2004).
- [33] G. Cognola, E. Elizalde, S. Nojiri, S. D. Odintsov and S. Zerbini, *Phys. Rev. D* **73**, 084007 (2006).
- [34] S. Capozziello, V. F. Cardone, E. Elizalde, S. Nojiri and S. D. Odintsov, *Phys. Rev. D* **73**, 043512 (2006).
- [35] E. Elizalde and P. J. Silva, *Phys. Rev. D* **78**, 061501 (2008).
- [36] S. D. Odintsov and V. K. Oikonomou, *Class. Quant. Grav.* **36** (2019) 065008.

- [37] S. Nojiri, S. D. Odintsov and V. K. Oikonomou, Nucl. Phys. B **941** (2019) 11.
- [38] P. Shah and G. C. Samanta, Eur. Phys. J. C **79** (2019) 414.
- [39] G. C. Samanta and N. Godani, Mod. Phys. Lett. A, Accepted (2019).
- [40] N. Godani and G. C. Samanta, Mod. Phys. Lett. A, Accepted (2019)
- [41] T. Chiba, Phys. Lett. B **575**, 1 (2003).
- [42] G. Cognola, E. Elizalde, S. Nojiri, S. D. Odintsov, L. Sebastiani and S. Zerbini, Phys. Rev. D **77** (2008) 046009.
- [43] S. Nojiri and S. D. Odintsov, Phys. Rev. D **77** (2008) 026007.
- [44] S. Nojiri and S. D. Odintsov, Phys. Lett. B **659**, 821 (2008).
- [45] T. Harko, F. S. N. Lobo, S. Nojiri and S. D. Odintsov, Phys. Rev. D **84** (2011) 024020.
- [46] M. J. S. Houndjo, Int. J. Mod. Phys. D **21** (2012) 1250003.
- [47] M. Sharif and M. Zubair, JCAP **1203** (2012) 028.
- [48] M. Jamil, D. Momeni, M. Raza and R. Myrzakulov, Eur. Phys. J. C **72** (2012) 1999.
- [49] F. G. Alvarenga, A. de la Cruz-Dombriz, M. J. S. Houndjo, M. E. Rodrigues and D. Sàez-Gómez, Phys. Rev. D **87** (2013) 103526.
- [50] A. F. Santos, Mod. Phys. Lett. A **28** (2013) 1350141.
- [51] G. C. Samanta, Int. J. Theor. Phys. **52** (2013) 2303.
- [52] H. Shabani and M. Farhoudi, Phys. Rev. D **88** (2013) 044048.
- [53] R. L. Naidu, D. R. K. Reddy, T. Ramprasad and K. V. Ramana, Astrophys. Space Sci. **348** (2013) 247.
- [54] G. C. Samanta and S. N. Dhal, Int. J. Theor. Phys. **52** (2013) 1334.
- [55] S. Chandel and S. Ram, Indian J. Phys. **87** (2013) 1283.
- [56] G. C. Samanta, Int. J. Theor. Phys. **52** (2013) 2647.
- [57] H. Shabani and M. Farhoudi, Phys. Rev. D **90** (2014) 044031.
- [58] G. C. Samanta, S. Jaiswal and S. K. Biswal, Eur. Phys. J. Plus **129** (2014) 48.
- [59] P. H. R. S. Moraes, Eur. Phys. J. C **75** (2015) 168.
- [60] I. Noureen and M. Zubair, Eur. Phys. J. C **75** (2015) 62.
- [61] M. Farasat Shamir, Eur. Phys. J. C **75** (2015) 354.

- [62] B. Mirza and F. Oboudiat, *Int. J. Geom. Meth. Mod. Phys.* **13** (2016) 1650108.
- [63] R. A. C. Correa and P. H. R. S. Moraes, *Eur. Phys. J. C* **76** (2016) 100.
- [64] G. Ramesh and S. Umadevi, *Astrophys. Space Sci.* **361** (2016) 2.
- [65] P. H. R. S. Moraes and R. A. C. Correa, *Astrophys. Space Sci.* **361** (2016) 91.
- [66] P. H. R. S. Moraes, Jose D. V. Arbañil and M. Malheiro, *JCAP* **1606** (2016) 005.
- [67] R. Zaregonbadi, M. Farhoudi and N. Riazi, *Phys. Rev. D* **94** (2016) 084052.
- [68] A. Das, F. Rahaman, B. K. Guha and S. Ray, *Eur. Phys. J. C* **76** (2016) 654.
- [69] B. Mishra, S. Tarai and S. K. Tripathy, *Adv. High Energy Phys.* **2016** (2016) 8543560.
- [70] Z. Yousaf, K. Bamba and M. Z. ul Haq Bhatti, *Phys. Rev. D* **93** (2016) 124048.
- [71] G. C. Samanta, R. Myrzakulov and Parth Shah, *Z. Naturforsch. A* **72** (2017) 365.
- [72] N. Godani, *Int. J. Geom. Meth. Mod. Phys.* **16** (2018) 1950024.
- [73] E. Elizalde and M. Khurshudyan, *Phys. Rev. D* **98** (2018) 123525.
- [74] Y. Aditya and D. R. K. Reddy, *Astrophys. Space Sci.* **364** (2019) 3.
- [75] E. Elizalde and M. Khurshudyan, *Phys. Rev. D* **99** (2019) 024051.
- [76] T. M. Ordines and E. D. Carlson, *Phys. Rev. D* **99** (2019) 104052.
- [77] L. D. Landau and E. M. Lifshitz, *The Classical Theory of Fields*, Butterworth-Heinemann, Oxford (1998).
- [78] C. Molina-Paris and M. Visser, *Phys. Lett. B* **455** (1999) 90.
- [79] Yi-Fu Cai, T. Qiu, X. Zhang, Y. Song Piao and M. Li, *JHEP*, **0710** (2007) 071.
- [80] S. D. Odintsov, V. K. Oikonomou and E. N. Saridakis, *Annals Phys.* **363** (2015) 141.
- [81] S. D. Odintsov and V. K. Oikonomou, *Phys. Rev. D* **91** (2015) 064036.
- [82] S. D. Odintsov and V. K. Oikonomou, *Phys. Rev. D* **92** (2015) 024016.
- [83] S. D. Odintsov and V. K. Oikonomou, *Int. J. Mod. Phys. D* **26** (2017) 1750085.
- [84] Planck Collaboration, *Astron. Astrophys.* **594** (2016).
- [85] R. Jimenez, L. Verde, T. Treu, and D. Stern, *ApJ* **593** (2003) 622.
- [86] J. Simon, L. Verde, and R. Jimenez, *Phys. Rev. D* **71** (2005) 123001.
- [87] D. Stern et al., *J. Cosmol. Astropart. Phys.* **2** (2010) 008.

- [88] M. Moresco et al., *J. Cosmol. Astropart. Phys.* **8** (2012) 006.
- [89] C. Blake et al., *Mon. Not. R. Astron. Soc.* **425**(2012) 405-414.
- [90] C. Zhang et al., *Res. Astron. Astrophys.* **14** (2014) 121.
- [91] M. Moresco, *Mon. Not. R. Astron. Soc.* **450** (2015) L16-L20.
- [92] T. Delubac et al., *Astron. Astrophys.* **574** (2015) A59.

Table 1: Hubble Parameter Observational data

S.No.	z	$H(z)$	σ_i	Reference
1	.090	69	12	[85]
2	.17	83	8	[86]
3	.27	77	14	[86]
4	.4	95	17	[86]
5	.9	117	23	[86]
6	1.3	168	17	[86]
7	1.43	177	18	[86]
8	1.53	140	14	[86]
9	1.75	202	40	[86]
10	.48	97	62	[87]
11	.88	90	40	[87]
12	.179	75	4	[88]
13	.199	75	5	[88]
14	.352	83	14	[88]
15	.593	104	13	[88]
16	.68	92	8	[88]
17	.781	105	12	[88]
18	.875	125	17	[88]
19	1.037	154	20	[88]
20	.44	82.6	7.8	[89]
21	.60	87.9	6.1	[89]
22	.73	97.3	7	[89]
23	.07	69	19.6	[90]
24	.12	68.6	26.2	[90]
25	.2	72.9	29.6	[90]
26	.28	88.8	36.6	[90]
27	1.363	160	33.6	[91]
28	1.965	186.5	50.4	[91]
29	2.34	222	7	[92]